nuhep-th/22-03
FERMILAB-PUB-22-364-T

Timing and Multi-Channel: Novel Method for Determining the Neutrino Mass Ordering from Supernovae

Vedran Brdar[1,2,a] and Xun-Jie Xu[3,b]

[1] *Fermi National Accelerator Laboratory, Batavia, IL 60510, USA*
[2] *Northwestern University, Dept. of Physics & Astronomy, Evanston, IL 60208, USA*
[3] *Institute of High Energy Physics, Chinese Academy of Sciences, Beijing 100049, China*

One of the few remaining unknowns in the standard three-flavor neutrino oscillation paradigm is the ordering of neutrino masses. In this work we propose a novel method for determining neutrino mass ordering using the time information on early supernova neutrino events. In a core-collapse supernova, neutrinos are produced earlier than antineutrinos and, depending on the mass ordering which affects the adiabatic flavor evolution, may cause earlier observable signals in ν_e detection channels than in others. Hence, the time differences are sensitive to the mass ordering. We find that using the time information on the detection of the first galactic supernova events at future detectors like DUNE, JUNO and Hyper-Kamiokande, the mass ordering can already be determined at 2σ CL, while $\mathcal{O}(10)$ events suffice for the discovery. Our method does not require high-statistics and could be used within the supernova early warning system (SNEWS) which will have access to the time information on early supernova neutrino events recorded in a number of detectors. The method proposed in this paper also implies a crucial interplay between the mass ordering and the triangulation method for locating supernovae.

1 Introduction

The discovery of neutrino oscillations [1–3], as one of the most relevant scientific achievements in the last few decades, has undoubtedly established that neutrinos are massive particles. Neutrino oscillation probabilities are functions of neutrino mass squared differences which are precisely known by now [4]. However, the ordering of these masses is still unknown; namely, it is not yet established whether the neutrino mass eigenstate which comprises the largest fraction of electron neutrino flavor is the lightest one. If so, the neutrino mass ordering is dubbed "normal" (NO), while the alternative option is the "inverted" ordering (IO).

There are several multi-billion dollar experiments that will start operating by the end of the decade, namely DUNE [5], Hyper-Kamionade [6] and JUNO [7] and they are all expected to have the capability to probe neutrino mass ordering [5, 8, 9]. As an alternative to man-made neutrinos from reactor and acceleration facilities, neutrinos from core-collapse supernove (SNe) can also be employed for the determination of mass ordering. Unlike for the case of SN 1987A [10] from which only a handful of neutrinos were detected [11], the above mentioned experiments will be able to collect thousands of events from the next galactic supernova via several different interaction channels.

Neutrinos from supernovae were already suggested in the context of neutrino mass ordering determination [12–14]. One of the methods previously discussed was to focus on neutrinos produced in the neutronization burst and to use event counts from the interaction of electron neutrinos (ν_e) in detectors such as DUNE that excel at ν_e detection. Due to matter effects in SNe [15–17], the survival probability of ν_e is higher and leads to more ν_e events in IO when compared to the NO scenario. Along similar lines, following the neutronization burst, electron antineutrinos ($\overline{\nu}_e$) will start to be produced in significant amounts and the matter effects in this case also affect the flux of $\overline{\nu}_e$, making

[a] vbrdar@fnal.gov
[b] xuxj@ihep.ac.cn

This manuscript has been authored by Fermi Research Alliance, LLC under Contract No. DE-AC02-07CH11359 with the U.S. Department of Energy, Office of Science, Office of High Energy Physics.

NO and IO scenarios distinguishable in experiments like Super/Hyper-Kamiokande and JUNO that utilize inverse beta decay (IBD). Other interesting approaches include consideration of matter effects in Earth which lead to potentially detectable spectral distortions [18], or using differences in arrival times of neutrino mass eigenstates [19]. These approaches require either sufficiently high energy resolution or tremendously large-scale detectors. For a more detailed discussion on previously proposed techniques we refer the interested reader to the review [14].

In this paper we propose a novel method for determining the mass ordering based on the time differences between neutrino and antineutrino events from a galactic SN. Since early SN neutrinos are produced via neutronization, neutrinos are emitted from SN earlier than antineutrinos, leading to an observable time difference between neutrino and antineutrino detection channels. Initially being produced from neutronization as ν_e, the early neutrinos can be partially (IO) or almost entirely (NO) converted to ν_μ and ν_τ due to the adiabatic flavor evolution in the presence of matter effects [12]. Therefore, for ν_e events at e.g. DUNE, the first few events in the NO are delayed when comparing to the IO scenario. For $\overline{\nu}_e$, which can be well measured via the IBD process at JUNO and Super/Hyper-Kamiokande, the timing of the first few events is less affected by the mass ordering. Hence, the time difference between the onset of events at DUNE and IBD detectors, after subtracting corrections due to different geographical locations of experiments, provides a handle for the determination of the mass ordering — the larger it is, the likelihood for IO increases. Our method utilizes electron neutrinos produced already during the infall phase of SN. Although the statistics of events induced by such neutrinos is low, it is well-known that neutrino fluxes in this period are practically model independent, making any mass ordering statement quite robust. As we will show, even by comparing the time difference between the first ν_e and $\overline{\nu}_e$ events at DUNE and JUNO respectively, one can already determine the mass ordering at 2σ CL while only a handful of events are required to guarantee a discovery.

The method proposed in this paper can be particularly useful when incorporated in the supernova early warning system (SNEWS) [20] which should have access to the first few neutrino events from all involved detectors well before the full data set of each experiment becomes available. This means that besides not requiring high-statistics and being practically independent on the SN properties such as the progenitor mass, this method should be extremely time-efficient. In addition, we will show that this study is also helpful in the context of the triangulation method [21–23] that can be utilized for determining a SN location via inter-detector time differences.

The paper is organized as follows. In Section 2 we discuss SN fluxes for relevant (anti)neutrino flavors and compute respective event rates at various detectors. In Section 3 we first discuss statistical methods employed for assessing the timing of neutrino interactions and calculate expected time window for the occurrence of particular events. This allows us to compute the statistical significance for the discrimination between NO and IO for the method proposed in this paper. In Section 4 we discuss the non-trivial impact of the mass ordering on techniques proposed for determining SN location via triangulation. Finally, we conclude in Section 5.

2 Neutrino Event Rates and their dependence on the mass ordering

Neutrino fluxes from SNe are calculated from extensive simulations and results in this work are obtained using fluxes from the Garching group, see [24, 25]. Neutrino fluxes feature astrophysical uncertainties as well as potential contribution from flavor transitions induced by neutrino self-interactions [26]. During deleptonization phase of SNe where it is essentially only electron neutrinos that get produced, the effects from self-interactions are suppressed, particularly for the "standard" iron core SNe [27]; collective effects for such early neutrinos are non-existent [28]. The standard matter potential hence dominates and it induces the occurrence of two Mikheyev-Smirnov-Wolfenstein

resonances [15–17], corresponding to the atmospheric and solar mass squared differences, which neutrinos encounter while travelling outwards[1]. Provided the adiabatic evolution, the fluxes of neutrinos [12, 29] at distances much greater than the radius of the star read

$$\begin{aligned}
\Phi_{\nu_e} &= \Phi^0_{\nu_x}\,, \\
\Phi_{\bar{\nu}_e} &= \Phi^0_{\bar{\nu}_e}\cos^2\theta_{12} + \Phi^0_{\nu_x}\sin^2\theta_{12}\,, \\
\Phi_{\nu_x} &= \frac{1}{4}\left(2+\cos^2\theta_{12}\right)\Phi^0_{\nu_x} + \frac{1}{4}\Phi^0_{\nu_e} + \frac{1}{4}\Phi^0_{\bar{\nu}_e}\sin^2\theta_{12}\,,
\end{aligned} \tag{1}$$

for NO and

$$\begin{aligned}
\Phi_{\nu_e} &= \Phi^0_{\nu_e}\sin^2\theta_{12} + \Phi^0_{\nu_x}\cos^2\theta_{12}\,, \\
\Phi_{\bar{\nu}_e} &= \Phi^0_{\nu_x}\,, \\
\Phi_{\nu_x} &= \frac{1}{4}\left(2+\sin^2\theta_{12}\right)\Phi^0_{\nu_x} + \frac{1}{4}\Phi^0_{\bar{\nu}_e} + \frac{1}{4}\Phi^0_{\nu_e}\cos^2\theta_{12}\,,
\end{aligned} \tag{2}$$

for IO where θ_{12} stands for the solar mixing angle and ν_x represents fluxes of muon and tau (anti)neutrinos that are practically identical in SNe. The fluxes in Eqs. (1) and (2) follow inverse-square law; in this paper we assume galactic SN at the distance of $d = 10$ kpc from Earth. Φ^0 represents fluxes at distances closer to the center of the star than the two resonance regions. For Φ^0, we adopt parametrization from [30] involving the so called pinching parameter through which the deviation of neutrino distribution function from the Maxwell-Boltzmann one is quantified, as well as the neutrino luminosity, L, ($\Phi^0 \propto L$) that is a parameter commonly included in the output of SN simulations. In Fig. 1 we show neutrino luminosities for all neutrino flavors. In the left panel we focus on early times ($t < 20$ ms, where $t = 0$ is defined by the time of the core bounce) and it can be inferred that in this time window luminosities are practically model independent. To illustrate that, we employed four SN simulations from [24, 25], see also [22]. In contrast, in the right panel we show luminosities associated to the accretion and cooling phase; clearly, the theoretical uncertainties in this time window are much larger. The cutoff for SN3 and SN4 models arises because in those simulations star collapses into a black hole [31]. For our numerical calculations, we use model denoted as SN2, obtained by simulating the core-collapse of a 27 $M_\odot$ progenitor star. From the left panel it is obvious that electron neutrinos strongly dominate up to roughly 10 ms after the core bounce when neutronization burst [13] ends and we stress that it is precisely neutrinos produced in this time window that are crucial for the success of the method proposed in this work, as discussed below.

Following the transition of resonance regions, SN neutrinos that will be observed from this early emission will not be ν_e in case of NO (see again Eq. (1)). For IO, on the other hand, the difference between these early ν_e fluxes at smaller and larger distances (modulo inverse-square law dependence) with respect to resonance locations is only a factor of $\sin^2\theta_{12} \approx 0.25$. We illustrate that in Fig. 2. There, for each neutrino flavor (see particular panel) we show fluxes before (black) and after (orange for IO, blue for NO) encountering resonances. Focusing on the left panel it becomes clear that for a detector that will be particularly successful in detecting ν_e, more of early produced neutrinos will be detected if the mass ordering is IO. In turn, the onset of SN events in such a detector should occur earlier in time for IO.

DUNE is such an experiment that will predominantly detect SN ν_e via the charged-current process with Ar (ArCC): $\nu_e + {}^{40}\mathrm{Ar} \to e^- + {}^{40}\mathrm{K}^*$. In contrast, other large neutrino detectors like

[1] In contrast, matter effects from neutrino propagation in Earth are small and can be ignored [23].

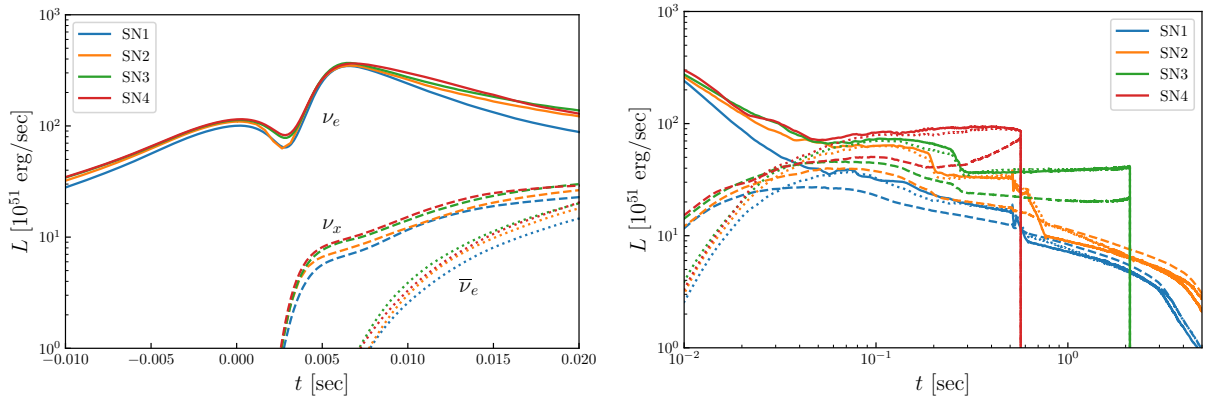

FIG. 1. Neutrino luminosity curves for four considered SN models [24, 25]. The left panel shows the period of infall and neutronization burst ($t < 20$ ms after the core bounce) and in this time window neutrino luminosities are rather model-independent. In contrast, the luminosities for particular flavor associated to the accretion and cooling stage of SN (right panel) feature larger discrepancies across the considered models.

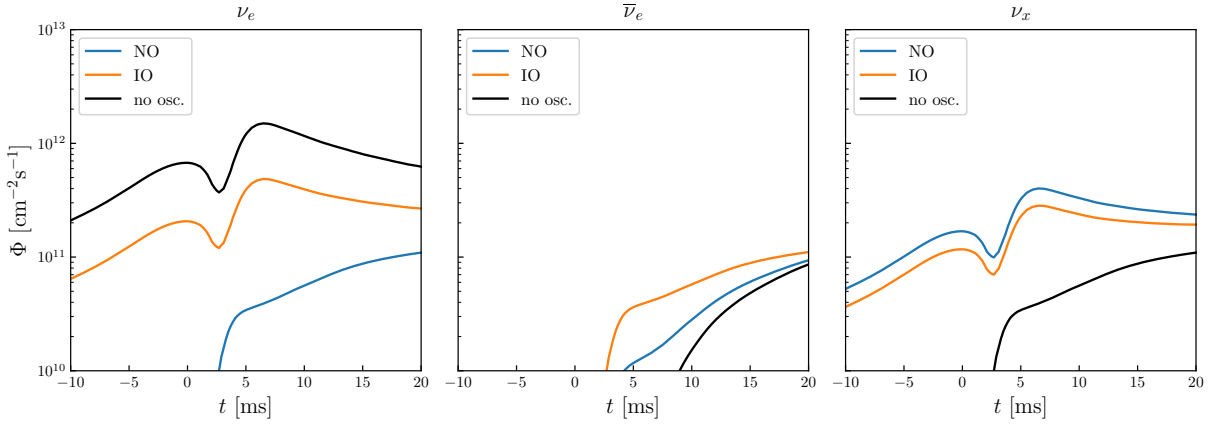

FIG. 2. Comparison between SN neutrino flux in NO (blue) and IO (orange) as well as in the absence of neutrino oscillations (black).

JUNO and Super/Hyper-Kamiokande have greater capability of detecting $\overline{\nu}_e$ via the IBD process. To investigate their capability for SN neutrino detection, we need to compute the event rates, determined by

$$R(t) = N_{\rm target} \int \Phi(E_\nu, t)\sigma(E_\nu)dE_\nu \,, \tag{3}$$

where $N_{\rm target}$ is the number of target particles in the detector and $\sigma(E_\nu)$ is the cross section for the detection process. We employ this formula for all channels and all (anti-)neutrino species by properly taking fluxes, cross sections and number of target particles for different detectors. Apart from the two dominant detection channels (ArCC and IBD), we also consider all-flavor neutrino-electron elastic scattering events (eEs) for the aforementioned detectors as well as neutrino-proton elastic scattering events (pES) for JUNO. The cross sections for eES and pES are taken from Refs. [32, 33]. The thresholds of electron recoil are set to 5, 0.2, and 5 MeV for DUNE, JUNO, and Super/Hyper-Kamiokande, respectively [34, 35]. As for pES, using the quenched energy deposit indicated in Fig. 5 in Ref. [32], we set the threshold of proton recoil at 1.2 MeV for JUNO. The

	N ($t < 20$ ms, NO)	N ($t < 20$ ms, IO)	N (total, NO)	N (total, IO)
DUNE-ArCC	11.3	50.9	3285	3097
DUNE-eES	2.99	6.48	311	314
JUNO-IBD	14.2	27.2	6297	6194
JUNO-eES	4.11	8.50	362	369
JUNO-pES	18.8	19.2	3670	3798
SuperK-IBD	17.6	33.8	7830	7701
SuperK-eES	2.95	6.39	307	310
HyperK-IBD	206	395	91517	90011
HyperK-eES	34.5	74.7	3588	3628

TABLE I. Number of events for indicated detectors and channels given in two time windows. In second (NO) and third (IO) column we focus on $t < 20$ ms while in the last two columns we show the total number of events associated to a SN explosion.

fiducial masses of DUNE, JUNO, and Super/Hyper-Kamiokande are set to 40, 20, and 32/374 kt respectively. For DUNE, such mass will be obtained by successively adding individual 10 kt modules at the far detector. In addition, in all our calculations we include background events [22]. With the above setup, we compute the expected number of galactic SN events for the aforementioned experiments; these are shown in Table I.

The main idea in this paper is to use both DUNE and JUNO or Super/Hyper-Kamiokande simultaneously in order to discover the mass ordering. Given the event rates in Table I, for IO there are clearly many more ArCC events in $t < 20$ ms window; this implies that for IO the first event recorded in the detector will occur earlier. For IBD channel, we do not see a dramatic difference between event counts across NO and IO for $t < 20$ ms. Therefore, the time difference between the onset of neutrino events at DUNE and at a given IBD detector will be larger for IO (after appropriately subtracting time of propagation in Earth for two detectors at different locations) and this is the reason how one can probe mass ordering by focusing only on timing of neutrino events. In Section 3 we will introduce statistical method for determination of the time of n-th neutrino event in the detector which will allow us to assess how many neutrino events are required in order to make interesting statistical statements on the mass ordering. Let us close this section by stating that in contrast to comparing ArCC and IBD events at different detectors one may be tempted to also compare interaction times of first few eES and ArCC at DUNE or eES and IBD at JUNO or Super/Hyper-Kamiokande, focusing hence on a single detector and two channels. This is possible since events from charged current scattering on nuclei and those from neutral current scattering on electrons can easily be distinguished from one another. While we will also show projections for such strategy in Section 3, we will eventually conclude that the most promising situation for determination of the ordering is still the case where two different detectors are involved.

3 Statistical Methods and Results

Let us consider the first event in a detector and denote the time of the occurrence of such an event by $t_{1\rm st}$. Given the expected event rate, $R(t)$, we would like to know the statistical expectation and fluctuation of $t_{1\rm st}$. Obviously, the first event is unlikely to appear in any $R(t)$-suppressed period. It is also unlikely to appear when the integrated event rate is too large ($\int^t R(t')dt' \gg 1$), because it implies that a large number of events should have already occurred. In Appendix A we have computed the probability density function (p.d.f) of $t_{1\rm st}$ which reads

$$p_{1\rm st}(t_{1\rm st}) = R(t_{1\rm st}) \exp\left[-\int_{-\infty}^{t_{1\rm st}} R(t)dt\right]. \tag{4}$$

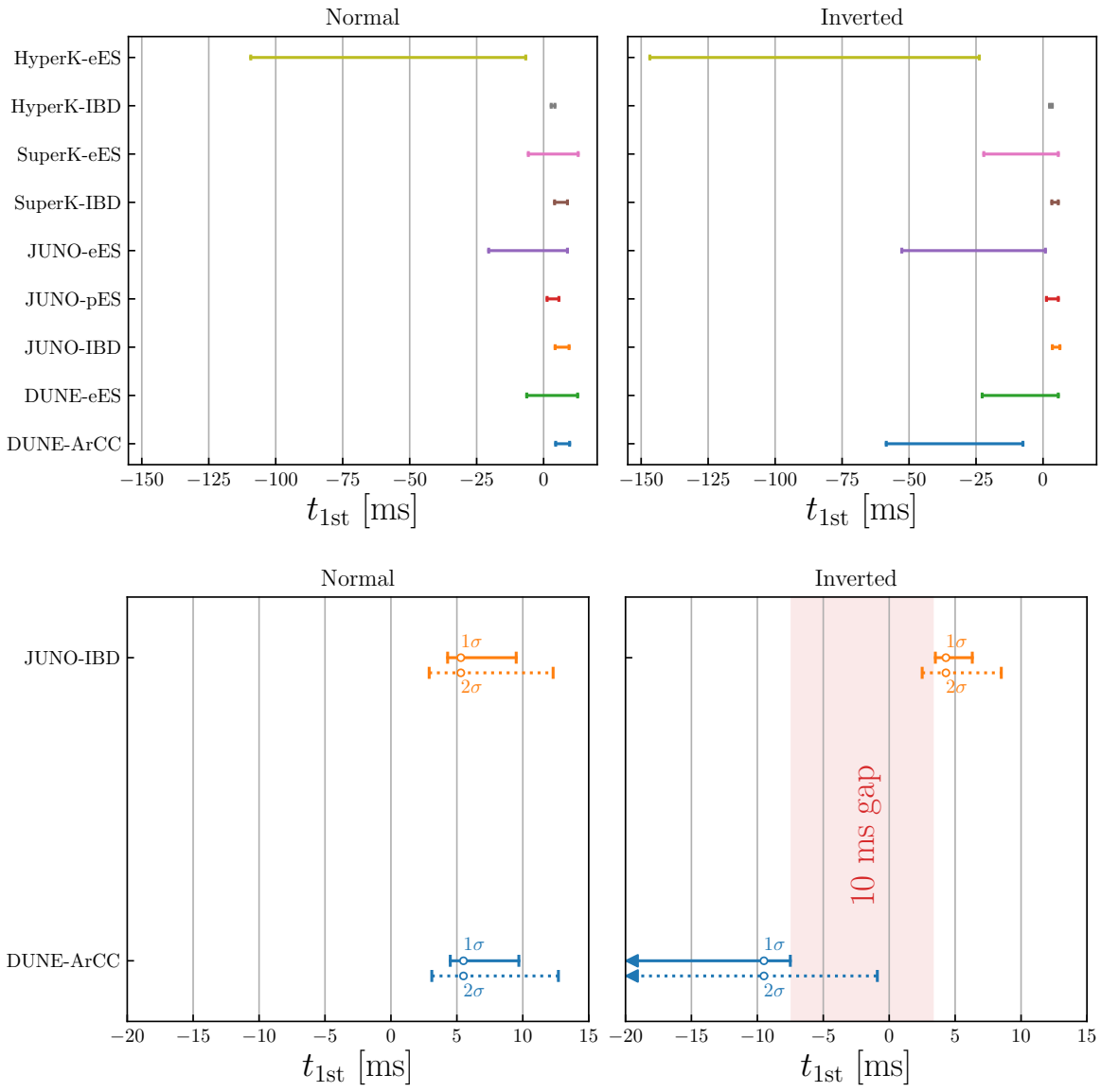

FIG. 3. Expected time window for the first event detection. The upper panels show 1σ uncertainty bars for the time of the first event detection ($t_{1\mathrm{st}}$) at DUNE, JUNO and Super/Hyper-Kamiokande via multiple detection channels including ArCC, IBD, eES, and pES. Left (right) panel is for NO (IO). Lower panels are dedicated to the comparison between JUNO-IBD and DUNE-ArCC to illustrate that the time separation between the respective first events is typically $\gtrsim 10$ ms in the IO, which would be a statistically significant signal for mass ordering. In lower panels we also show the maximal probability points (marked by "$\circ$") and 2σ uncertainty bars.

It is indeed suppressed when either the event rate is small or the integrated event rate is large.

Using Eq. (4), we can compute the expected interval of $t_{1\mathrm{st}}$ for specified CL. Denote the probability of $t_{1\mathrm{st}}$ occurring in $[t_-,\ t_+]$ by $1-\alpha$, where $\alpha = 0.3173$ (0.0455) for 1σ (2σ) CL. Then, the interval $[t_-,\ t_+]$ is determined by

$$\int_{-\infty}^{t_-} p_{1\mathrm{st}}(t)dt = \int_{t_+}^{\infty} p_{1\mathrm{st}}(t)dt = \frac{\alpha}{2}. \tag{5}$$

In the upper panels of Fig. 3, we show 1σ intervals of $t_{1\mathrm{st}}$ for all important detection channels in

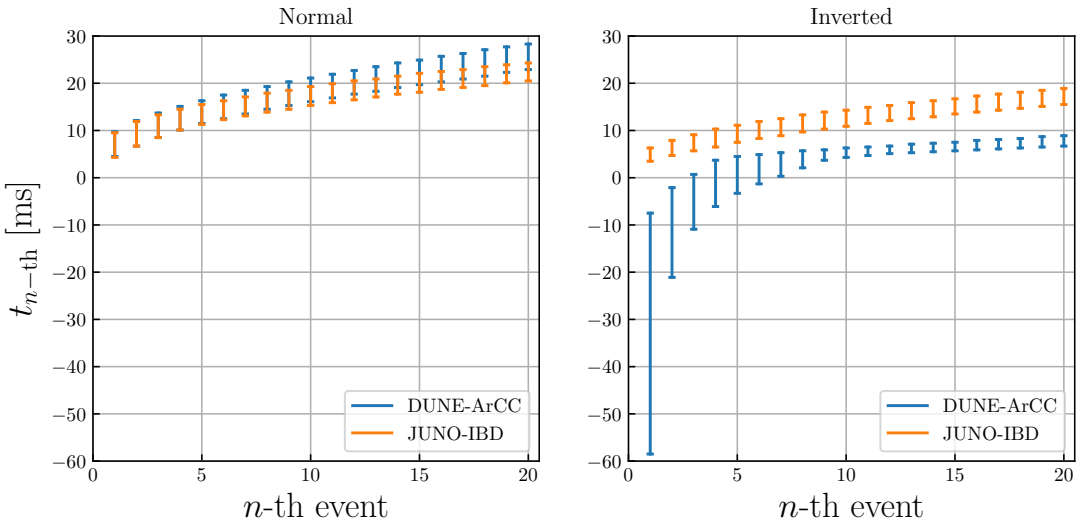

FIG. 4. The expected time of first 20 events at DUNE and JUNO in the ArCC and the IBD detection channels, respectively. Left (right) panel is for NO (IO).

DUNE, JUNO and Super-/Hyper-Kamiokande. One can see that the intervals for the IBD channel, through which only $\overline{\nu}_e$ are detected, are comparatively late and short in both NO and IO cases, while the ν_e-dedicated channel ArCC shows a significantly earlier interval in the IO. For pES, since the cross sections of neutrinos and anti-neutrinos are almost the same[2] and independent of flavors, the 1σ intervals in the NO and IO are nearly identical. For eES, neutrinos and anti-neutrinos of all flavors are detected and, due to the differences of cross sections ($\sigma_{\nu_e+e} > \sigma_{\overline{\nu}_e+e} > \sigma_{\nu_x+e} > \sigma_{\overline{\nu}_x+e}$), 1σ intervals are sensitive to mass ordering.

In the lower panels of Fig. 3, we concentrate on the comparison between DUNE-ArCC and JUNO-IBD measurements to further illustrate our method. As shown in the lower left panel, the 1σ intervals of $t_{1\text{st}}$ are very similar for NO: $t_{1\text{st}} \in [4.5, 9.7]$ ms for JUNO-IBD, and $[4.3, 9.5]$ ms for DUNE-ArCC. This implies that the time difference between the first events at JUNO-IBD and DUNE-ArCC in the NO case is likely to be less than ~ 5 ms at 1σ CL. In the IO case, as shown in the lower right panel, there is a significant gap between the 1σ intervals: $t_{1\text{st}} \in [3.5, 6.3]$ ms for JUNO-IBD and $[-58.5, -7.5]$ ms for DUNE-ArCC, which implies that the time difference should be greater than ~ 10 ms at 1σ CL. Note that, as a consequence of rapidly increasing event rates, the p.d.f of $t_{1\text{st}}$ is non-Gaussian and the maximal probability points are not in the middle of these intervals.

In order to obtain the statistical significance for discriminating between NO and IO reflected in Fig. 3, we shall inspect the statistics of the time difference of the first event ($\Delta t \equiv t^a_{1\text{st}} - t^b_{1\text{st}}$) between two experiments labelled as a and b. Given the p.d.f of $t^a_{1\text{st}}$ and $t^b_{1\text{st}}$, which are denoted by p_a and p_b respectively, the p.d.f of Δt is determined by (see Appendix A)

$$p_\Delta(\Delta t) = \int p_a\left(\frac{t+\Delta t}{2}\right) p_b\left(\frac{t-\Delta t}{2}\right)\frac{dt}{2}\,. \tag{6}$$

Using Eq. (6), we find that NO and IO scenarios are statistically discernible at 1.8σ CL by employing only the first SN events at JUNO-IBD and DUNE-ArCC.

Going beyond the first-event analysis, one can significantly improve the results by including more subsequent events. In Fig. 4, we show the 1σ intervals of $t_{n\text{-th}}$, which is defined as the time of the

[2] The difference between $\nu + p$ and $\overline{\nu} + p$ cross sections is suppressed by E_ν/m_p [32].

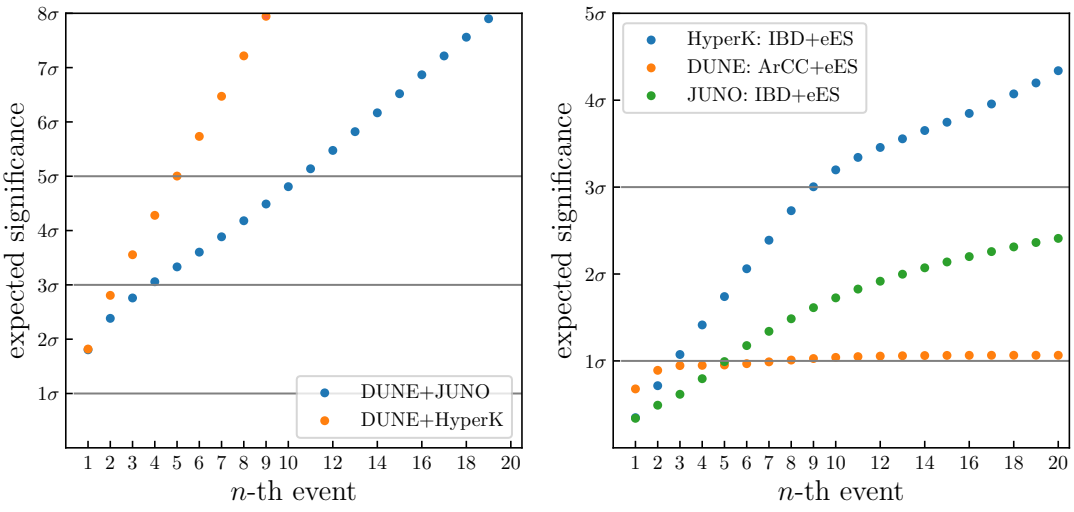

FIG. 5. Expected significance for neutrino mass ordering as a function of recorded number of events for which we only require the timing information. In the left panel, ArCC in DUNE and IBD in JUNO or Hyper-Kamiokande is considered. Knowing only the timing of the first event in these two channels, a 2σ statement can be made. For a discovery with DUNE+Hyper-Kamiokande (DUNE+JUNO) 5 (11) events suffice. In the right panel we compare charged current channel and neutrino-electron elastic scattering channel for all detectors separately and find that only at Hyper-Kamiokande $> 3\sigma$ statement can be made. This implies that the interplay of two different detectors by comparing respective dominant interaction channels (ArCC and IBD) is most successful for probing the mass ordering.

n-th event. For the first 20 events, DUNE-ArCC events will appear significantly earlier than JUNO-IBD ones in the IO case; in contrast, as discussed above, the timing in these two channels for NO is similar. Applying our method to the subsequent events and combining the statistical significance, we find that with the first 4 (11) events from DUNE-ArCC and JUNO-IBD, NO and IO can be distinguished at 3σ (5σ) CL — see the left panel in Fig. 5. The combination of DUNE-ArCC with SuperK-IBD leads to very similar results. If DUNE-ArCC is combined with HyperK-IBD, 5σ CL can be reached with the first five events.

In the above analyses, we assume that the time differences from geographical locations of detectors have been subtracted, which is feasible if the direction of the SN neutrino flux is known (e.g. if the SN has been optically observed or if its astronomical coordinates have been reconstructed from eES [36]). Even without knowing the direction, one can still compare two different channels in the same detector. In the right panel of Fig. 5, we show the results of combining IBD or ArCC with eES in a single detector. Since in each combination either ν_e or $\overline{\nu}_e$ detection is limited by low statistics of (anti)neutrino-electron scattering events, the capability of determining the mass ordering is weaker when compared to the inter-detector combinations. For IBD+eES in JUNO or ArCC+eES in DUNE, one can get $\sim 1\sigma$ significance with the first 5 events. For IBD+eES in Hyper-Kamiokande, due to its much higher statistics, 3σ significance can be reached with the first 9 events.

4 Interplay with SN Triangulation

The idea of SN triangulation, i.e. locating the position of the SN in the sky by using the time differences of onset of neutrino events across several detectors, was first discussed in [21] where the scepticism about this method was presented. The idea was, however, revived in [22] where it was

shown, using fluxes from modern SN simulations, that the statistical uncertainties at present and near future detectors are such that triangulation becomes feasible. It was found that the galactic SN can be located with $\lesssim 5^\circ$ in both declination and right ascension coordinates. Later, in Ref. [23] (see also [37, 38]), the success of triangulation was further verified and now this methods is one of the prominent goals of SNEWS [20].

Here we wish to briefly discuss the interplay between triangulation and mass ordering determination. As discussed in Section 3, the method that guarantees 5σ CL result for the mass ordering involves the usage of event time differences between different detectors such as DUNE and JUNO, or DUNE and Hyper-Kamiokande (see the left panel in Fig. 5). The actual measurement of such time differences should be corrected by the propagation time difference arising from different locations of detectors with respect to the SN. It is crucial to account for the propagation time difference because it can be as large as $\mathcal{O}(10)$ ms. For DUNE and JUNO (Hyper-Kamiokande), the distance between the two detectors is 10.2 $(8.4)\times 10^3$ km, respectively. If the SN direction is in alignment with the connection of the two detectors, then the geographical contribution to the time difference is 34 (28) ms. Since the triangulation method makes use of these time differences, one can envisage that triangulation and mass ordering determination would be considerably entangled.

One way to disentangle the two would be to make use of the angular dependence of interaction channels such as eES which can determine the direction up to a few degrees[3] [36]. Taking, e.g., 5° for the uncertainty of the direction, the geographical time difference can be determined with an uncertainty of ~ 2.6 ms, which would be a subdominant uncertainty when compared to the error bars in Fig. 4. Hence, our method in Section 3 for determination of the mass ordering is rather feasible.

Once the ordering is known, the triangulation method can be performed. Looking at Fig. 4, when considering the first few events, the statistical uncertainty of the n-th event time at DUNE is quite large for IO. The triangulation method advocated in [23] is based on the comparison of the time of first neutrino events in several detectors. This turns out to be inefficient for IO; in that case it is much more advantageous to skip the first event and focus on later events (for instance the 10th event has a much smaller uncertainty and is still arising from the period of neutronization). On the other hand, if various mass ordering measurements converge to NO, then the first-event method should be robust.

5 Summary and Conclusions

In this work we have proposed a novel method for determination of neutrino mass ordering using SN neutrinos. Compared to previous studies based on high-statistics measurement of SN neutrino fluxes, our method focuses exclusively on the time information on the first couple of events during the period of infall and neutronization burst. The neutrino fluxes in this period are known to be the least dependent on SN models (see Fig. 1).

The crucial point for the success of this approach is the synergy among several upcoming large detectors including DUNE, JUNO and Hyper-Kamiokande. In the case of IO, a large time gap (~ 10 ms) between the onset of SN events in DUNE and JUNO/Hyper-Kamiokande is expected (see Fig. 3) while for NO all aforementioned detectors should start recording events almost simultaneously, due to the suppressed flux of electron neutrinos produced in the infall phase of SN. We found that recording only the first $\mathcal{O}(10)$ events suffices for conclusive (5σ) determination of the mass ordering

[3] Another promising and potentially very precise method for determining the position of galactic supernova in the sky is by detecting photons via optical telescopes. However, there are obstacles such as the limited field of view of such telescopes [20]; note also that in scenarios where the core of a SN collapses into a black hole there is no optical signal.

while the time difference between the very first event at DUNE and IBD detectors is already enough for a 2σ statement, as shown in Fig. 5.

Our method can be readily incorporated in SNEWS which will have immediate access to the first few events from aforementioned detectors when the next galactic SN occurs. Provided the SN position is known from e.g. optical observations and/or from the observed angular dependence of neutrino interaction channels, the proposed method will allow SNEWS to determine mass ordering with these early events. We have also discussed the interplay between mass ordering and determination of the SN position in the sky via triangulation and argued that the triangulation method can be successfully performed following determination of the mass ordering.

Acknowledgements

We benefited greatly from discussions with Alexander Friedland, Shunsaku Horiuchi, Shirley Li and Shun Zhou. We are also grateful to Alec Habig for reading the final version of the manuscript. Fermilab is operated by the Fermi Research Alliance, LLC under contract No. DE-AC02-07CH11359 with the United States Department of Energy. This work was performed in part during KITP program "Neutrinos as a Portal to New Physics and Astrophysics". X.J.X is supported in part by the National Natural Science Foundation of China under Grant No. 12141501.

A The statistical uncertainties of early events

In this appendix, we derive the formula used to study the statistical fluctuation of the time of the first event, $t_{1\mathrm{st}}$, and then generalize it to the second, third and other early events that could be of importance to our analysis.

Given an event rate curve $R(t)$ like the one computed in Eq. (3), the expected number of events occurring before time t reads

$$\mu(t) = \int_{-\infty}^{t} R(t')dt' \,, \tag{A1}$$

where the lower bound does not necessarily need to correspond to $-\infty$; it can be any time below which $R(t')$ vanishes or is negligible. In an actual observation, one can only detect an integer number of events and the probability of detecting n events is governed by the Poisson distribution

$$P_\mu(n) = \frac{\mu^n}{n!} e^{-\mu} \,. \tag{A2}$$

The probability of the first event occurring within $[t,\ t+dt]$ should be the probability of *no* events occurring before t multiplied by the probability of *one* event in $[t,\ t+dt]$ interval

$$P\left(t_{1\mathrm{st}} \in [t,\ t+dt]\right) = P_\mu(0) P_{d\mu}(1) \,, \tag{A3}$$

where $d\mu = R(t)dt$ according to Eq. (A1).

Substituting Eq. (A2) into Eq. (A3) we obtain the probability density function of $t_{1\mathrm{st}}$

$$p_{1\mathrm{st}}(t_{1\mathrm{st}}) = R(t_{1\mathrm{st}}) \exp\left[-\int_{-\infty}^{t_{1\mathrm{st}}} R(t)dt\right] . \tag{A4}$$

Note that

$$\int_{-\infty}^{t} p_{1\mathrm{st}}(t_{1\mathrm{st}})dt_{1\mathrm{st}} = 1 - e^{-\mu} \,, \tag{A5}$$

which is expected since the left-hand side corresponds to the probability of the first event occurring before t while $e^{-\mu} = P_\mu(0)$ on the right-hand side is the probability of no events occurring before t. The two probabilities should be complementary to each other.

Next, let us generalize Eq. (A4) to the case of the second event, for which the time is denoted by $t_{2\text{nd}}$. The probability of the second event occurring within $[t,\ t+dt]$ should be the probability that one (and only one) event has occurred before t multiplied by the probability of one event occurring within $[t,\ t+dt]$

$$P\left(t_{2\text{nd}} \in [t,\ t+dt]\right) = P_\mu(1) P_{d\mu}(1)\,. \tag{A6}$$

This gives

$$p_{2\text{nd}}(t_{2\text{nd}}) = \mu(t_{2\text{nd}}) \exp\left[-\mu(t_{2\text{nd}})\right] R(t_{2\text{nd}})\,. \tag{A7}$$

Further generalizations to the n-th event are straightforward. The probability density function of $t_{n\text{-th}}$ reads

$$p_{n\text{-th}}(t_{n\text{-th}}) = \frac{\mu(t_{n\text{-th}})^{n-1}}{(n-1)!} \exp\left[-\mu(t_{n\text{-th}})\right] R(t_{n\text{-th}})\,. \tag{A8}$$

Similar to Eq. (A5), the integral of $p_{n\text{-th}}(t_{n\text{-th}})$ can be calculated analytically

$$\int_{-\infty}^{t} p(t_{n\text{-th}}) dt_{n\text{-th}} = 1 - \frac{\Gamma(n,\mu)}{(n-1)!}\,, \tag{A9}$$

where $\Gamma(n,\mu)$ is the incomplete gamma function.

For two independent events (e.g. first events occurring at two detectors), given their respective probability density functions $p_a(t_a)$ and $p_b(t_b)$, the probability density function of $t_- = t_a - t_b$ can be obtained by the transformation of random variables: $(t_a,\ t_b) \to (t_-,\ t_+) \equiv (t_a - t_b,\ t_a + t_b)$. Including the Jacobian in this transformation ($dt_- dt_+ = 2 dt_a dt_b$), the probability density function of t_- reads

$$p_-(t_-) = \int p_a(t_a) p_b(t_b) \frac{dt_+}{2} = \int p_a\left(\frac{t_+ + t_-}{2}\right) p_b\left(\frac{t_+ - t_-}{2}\right) \frac{dt_+}{2}\,. \tag{A10}$$

[1] **Super-Kamiokande Collaboration**, Y. Fukuda *et al.*, *Evidence for oscillation of atmospheric neutrinos*, *Phys. Rev. Lett.* **81** (1998) 1562–1567, [hep-ex/9807003].

[2] **SNO Collaboration**, Q. R. Ahmad *et al.*, *Direct evidence for neutrino flavor transformation from neutral current interactions in the Sudbury Neutrino Observatory*, *Phys. Rev. Lett.* **89** (2002) 011301, [nucl-ex/0204008].

[3] **KamLAND Collaboration**, K. Eguchi *et al.*, *First results from KamLAND: Evidence for reactor anti-neutrino disappearance*, *Phys. Rev. Lett.* **90** (2003) 021802, [hep-ex/0212021].

[4] I. Esteban, M. C. Gonzalez-Garcia, M. Maltoni, T. Schwetz, and A. Zhou, *The fate of hints: updated global analysis of three-flavor neutrino oscillations*, *JHEP* **09** (2020) 178, [2007.14792].

[5] **DUNE Collaboration**, R. Acciarri *et al.*, *Long-Baseline Neutrino Facility (LBNF) and Deep Underground Neutrino Experiment (DUNE): Conceptual Design Report, Volume 1: The LBNF and DUNE Projects*, 1601.05471.

[6] **Hyper-Kamiokande Collaboration**, K. Abe *et al.*, *Hyper-Kamiokande Design Report*, 1805.04163.

[7] **JUNO Collaboration**, F. An *et al.*, *Neutrino Physics with JUNO*, *J. Phys. G* **43** (2016), no. 3 030401, [1507.05613].

[8] **Hyper-Kamiokande Collaboration**, J. Bian *et al.*, *Hyper-Kamiokande Experiment: A Snowmass White Paper*, in *2022 Snowmass Summer Study*, 3, 2022. 2203.02029.

[9] D. V. Forero, S. J. Parke, C. A. Ternes, and R. Z. Funchal, *JUNO's prospects for determining the neutrino mass ordering*, *Phys. Rev. D* **104** (2021), no. 11 113004, [2107.12410].

[10] N. Panagia, *SN 1987A: The Unusual explosion of a normal type II supernova*, *ASP Conf. Ser.* **342** (2005) 78, [astro-ph/0410275].

[11] **Kamiokande-II Collaboration**, K. Hirata *et al.*, *Observation of a Neutrino Burst from the Supernova SN 1987a*, *Phys. Rev. Lett.* **58** (1987) 1490–1493.

[12] A. S. Dighe and A. Yu. Smirnov, *Identifying the neutrino mass spectrum from the neutrino burst from a supernova*, *Phys. Rev.* **D62** (2000) 033007, [hep-ph/9907423].

[13] M. Kachelriess, R. Tomas, R. Buras, H. T. Janka, A. Marek, and M. Rampp, *Exploiting the neutronization burst of a galactic supernova*, *Phys. Rev.* **D71** (2005) 063003, [astro-ph/0412082].

[14] K. Scholberg, *Supernova Signatures of Neutrino Mass Ordering*, *J. Phys.* **G45** (2018), no. 1 014002, [1707.06384].

[15] L. Wolfenstein, *Neutrino Oscillations in Matter*, *Phys.Rev.* **D17** (1978) 2369–2374.

[16] S. P. Mikheev and A. Yu. Smirnov, *Resonance Amplification of Oscillations in Matter and Spectroscopy of Solar Neutrinos*, *Sov. J. Nucl. Phys.* **42** (1985) 913–917. [Yad. Fiz.42,1441(1985)].

[17] S. P. Mikheev and A. Yu. Smirnov, *Resonant amplification of neutrino oscillations in matter and solar neutrino spectroscopy*, *Nuovo Cim.* **C9** (1986) 17–26.

[18] E. Borriello, S. Chakraborty, A. Mirizzi, P. D. Serpico, and I. Tamborra, *(Down-to-)Earth matter effect in supernova neutrinos*, *Phys. Rev. D* **86** (2012) 083004, [1207.5049].

[19] J. Jia, Y. Wang, and S. Zhou, *On the Possibility to Determine Neutrino Mass Hierarchy via Supernova Neutrinos with Short-Time Characteristics*, *Chin. Phys. C* **43** (2019), no. 9 095102, [1709.09453].

[20] **SNEWS Collaboration**, S. Al Kharusi *et al.*, *SNEWS 2.0: a next-generation supernova early warning system for multi-messenger astronomy*, *New J. Phys.* **23** (2021), no. 3 031201, [2011.00035].

[21] J. F. Beacom and P. Vogel, *Can a supernova be located by its neutrinos?*, *Phys. Rev.* **D60** (1999) 033007, [astro-ph/9811350].

[22] V. Brdar, M. Lindner, and X.-J. Xu, *Neutrino astronomy with supernova neutrinos*, *JCAP* **04** (2018) 025, [1802.02577].

[23] N. B. Linzer and K. Scholberg, *Triangulation Pointing to Core-Collapse Supernovae with Next-Generation Neutrino Detectors*, *Phys. Rev. D* **100** (2019), no. 10 103005, [1909.03151].

[24] L. Hüdepohl. PhD thesis, Technische Universität München, 2013.

[25] A. Mirizzi, I. Tamborra, H.-T. Janka, N. Saviano, K. Scholberg, R. Bollig, L. Hudepohl, and S. Chakraborty, *Supernova Neutrinos: Production, Oscillations and Detection*, *Riv. Nuovo Cim.* **39** (2016), no. 1-2 1–112, [1508.00785].

[26] H. Duan, G. M. Fuller, and Y.-Z. Qian, *Collective Neutrino Oscillations*, *Ann. Rev. Nucl. Part. Sci.* **60** (2010) 569–594, [1001.2799].

[27] H. Duan, G. M. Fuller, J. Carlson, and Y.-Z. Qian, *Flavor Evolution of the Neutronization Neutrino Burst from an O-Ne-Mg Core-Collapse Supernova*, *Phys. Rev. Lett.* **100** (2008) 021101, [0710.1271].

[28] S. Hannestad, G. G. Raffelt, G. Sigl, and Y. Y. Y. Wong, *Self-induced conversion in dense neutrino gases: Pendulum in flavour space*, *Phys. Rev. D* **74** (2006) 105010, [astro-ph/0608695]. [Erratum: Phys.Rev.D 76, 029901 (2007)].

[29] J.-S. Lu, Y.-F. Li, and S. Zhou, *Getting the most from the detection of Galactic supernova neutrinos in future large liquid-scintillator detectors*, *Phys. Rev.* **D94** (2016), no. 2 023006, [1605.07803].

[30] M. T. Keil, G. G. Raffelt, and H.-T. Janka, *Monte Carlo study of supernova neutrino spectra formation*, *Astrophys. J.* **590** (2003) 971–991, [astro-ph/0208035].

[31] J. F. Beacom, R. N. Boyd, and A. Mezzacappa, *Black hole formation in core collapse supernovae and time-of-flight measurements of the neutrino masses*, *Phys. Rev.* **D63** (2001) 073011, [astro-ph/0010398].

[32] J. F. Beacom, W. M. Farr, and P. Vogel, *Detection of supernova neutrinos by neutrino proton elastic scattering*, *Phys. Rev.* **D66** (2002) 033001, [hep-ph/0205220].

[33] C. Giunti and C. W. Kim, *Fundamentals of Neutrino Physics and Astrophysics*. Oxford University Press, 2007.

[34] F. Capozzi, S. W. Li, G. Zhu, and J. F. Beacom, *DUNE as the Next-Generation Solar Neutrino*

Experiment, *Phys. Rev. Lett.* **123** (2019), no. 13 131803, [1808.08232].

[35] H.-L. Li, Y.-F. Li, M. Wang, L.-J. Wen, and S. Zhou, *Towards a complete reconstruction of supernova neutrino spectra in future large liquid-scintillator detectors*, *Phys. Rev. D* **97** (2018), no. 6 063014, [1712.06985].

[36] **Super-Kamiokande Collaboration**, K. Abe *et al.*, *Real-Time Supernova Neutrino Burst Monitor at Super-Kamiokande*, *Astropart. Phys.* **81** (2016) 39–48, [1601.04778].

[37] T. Mühlbeier, H. Nunokawa, and R. Zukanovich Funchal, *Revisiting the Triangulation Method for Pointing to Supernova and Failed Supernova with Neutrinos*, *Phys. Rev.* **D88** (2013) 085010, [1304.5006].

[38] A. Coleiro, M. Colomer Molla, D. Dornic, M. Lincetto, and V. Kulikovskiy, *Combining neutrino experimental light-curves for pointing to the next galactic core-collapse supernova*, *Eur. Phys. J. C* **80** (2020), no. 9 856, [2003.04864].